Influence of Long-Chain Branching on the Crystallization and Melting Behavior of Polycarbonates in Supercritical CO_2

Wentao Zhai,[†,‡] Jian Yu,*[,†] Weiming Ma,[†,‡] and Jiasong He*[,†]

Beijing National Laboratory for Molecular Sciences (BNLMS), Key Laboratory of Engineering Plastics, Joint Laboratory of Polymer Science and Materials, Institute of Chemistry, Chinese Academy of Sciences, Beijing 100080, China, and Graduate School, Chinese Academy of Sciences, Beijing 100039, China

Received September 19, 2006; Revised Manuscript Received November 7, 2006

ABSTRACT: The crystallization behavior of two long-chain branched bisphenol A polycarbonates (PC-Bs) was studied in supercritical CO_2 using differential scanning calorimetry (DSC), wide-angle X-diffraction, and atomic force microscopy (AFM), with a linear polycarbonate (PC-L) as reference. All the PCs had similar molecular weights and molecular weight distributions. Positron annihilation lifetime spectroscopy measurement indicated that the increase in free volume fraction of 13.1% (PC-B1) and 11.8% (PC-B2) was obtained with incorporating long-chain branches compared to PC-L. This increased segmental mobility decreased the energy barrier for PC crystallization and hence increased the crystallization kinetics for PC-Bs. Two melting peaks (T_{m1} and T_{m2}) observed during DSC heating scan were associated with the melting of secondary and primary crystallization, respectively. The T_{m2} of PC-Bs was about 2−4 °C lower than that of PC-L of at the same treatment time, pressure, and temperature. These results, qualitatively consistent with AFM results, mean that the incorporation of long-chain branches decreased the perfection or increased the lattice disorder of primary crystallites. The T_{m1} of crystallized PC-Bs was also much lower than that of PC-L under the same treatment conditions, which was attributed to the decrease in primary crystallization process and the resultant reduction in conformational constraints in the residual amorphous regions. AFM results also indicate that the branching structure might increase the crystallite density and sequentially the crystallinity degree of PC-Bs.

1. Introduction

For polymer materials, especially for polymers with regular chain structures, the crystallization is a general phenomenon and a very important process in industry because it controls the structural formation of the polymer and thereby strongly influences the properties of the final products.[1] Numerous researchers have verified that the branching structure such as branch length, branch content, and branch distribution affects the crystallization behavior of polymers. Among these branched polymers, the typical example is polyolefin due to easily tailored microstructure by metallocene and other "single-site" catalyst polymerizations.[2−4] These investigations have found the incorporation of short branches into linear polyolefin reduces its melting point and crystallinity because the branch points are always rejected to the folded surface of the lamellar structure as a defect. While for the long-chain branched polymer, the cocrystallization between main and side chains tends to increase the crystallinity. The introduction of branching structure in polyesters,[5] such as poly(ethylene terephthalate),[6,7] poly(L-lactic acid),[8,9] and poly(ϵ-caprolactone),[10,11] also affects their crystallization behavior compared to their corresponding linear structure. Usually, there is a critical branching concentration to affect the crystallization behavior of polyesters. Above the critical concentration, it is found that the crystallization rate decreases with increasing the branching concentration due to the added molecular entanglement restricting the segmental motions of the polymer.[6,7] Influences of the branched structure on crystallization behavior have also been observed in other polymers such as polyamides,[12,13] polyimides,[14] and polythiophenes.[15,16] Despite many polymer systems having been investigated, however, to our knowledge, there is no report on the crystallization behavior of bisphenol A polycarbonate (PC) with branched structure.

In our previous paper,[17] it was found that the long-chain branched PC exhibited higher melt strength and shear sensitivity compared to the linear one because the branch structure was long enough to form molecular entanglement. The dielectric relaxation analysis further indicated the branched PC possessed high molecular motion ability. The number of repeat units of branch chain for the branched PC was about 39.[17] This value was much larger than the needed chain length, 8−10 carbon atoms, for the side chain crystallization of alkyl-substituted polymer, such as linear low-density polyethylene,[18−20] poly(*n*-alkyl acrylates),[21] and poly(*n*-alkyl methacrylates).[21,22] Thus, the branch chain of PC would take part in crystallization, and the formed crystallites might act as the nucleation sites for PC crystallization. This enhanced nucleation correlated with the increased segmental mobility would significantly affect the crystallization behavior of PC.

It is widely accepted that PC exhibits very low crystallization kinetics. At the atmospheric pressure, PC has an induced period of about 170 h in thermal crystallization at 190 °C. A reason for the slow kinetics of crystal growth is the chain rigidity,[23] resulting in the high work of chain folding for PC (27.3 vs 5.7 kcal/mol for polyethylene).[24] Further evidence that segmental mobility controls the rate of PC crystallization is gained from the observed enhancement in crystallization rate when the sample is exposed to solvents or vapors because of the strong plasticization effect of solvent.[25,26] Solvent-induced crystallization of PC proceeds rapidly, the shorter treatment time of several minutes or hours contrary to thermal-induced crystallization. However, organic solvents are very difficult to remove com-

† Institute of Chemistry.
‡ Graduate School.
* Corresponding authors: E-mail: yuj@iccas.ac.cn, hejs@iccas.ac.cn, Fax: +86-10-8261 2857.

10.1021/ma062181g CCC: $37.00 © 2007 American Chemical Society
Published on Web 12/14/2006

Table 1. Characteristics of the PCs

sample	M_w (g/mol)	M_w/M_n	branching agent contents (mol %)	T_g (°)
PC-L	35 500	3.03		154.5
PC-B1	34 100	3.72	0.5	150.2
PC-B2	34 700	3.79	0.5	151.0

Scheme 1. Chemical Structures of the Different Branching Agents for PC-Bs

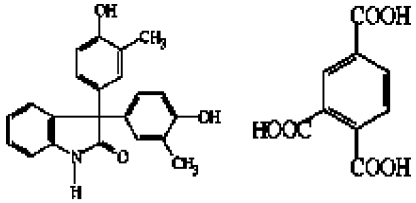

PC-B1 PC-B2

pletely after crystallization and less environmentally friendly as well.

CO_2 is a readily available, inexpensive, and environmentally benign gas. It exhibits tunable liquidlike solubility and gaslike viscosity under supercritical fluid conditions, which can be readily accessed due to its relatively low critical point at T_c = 31.1 °C and P_c = 7.37 MPa. It has shown that supercritical CO_2 ($scCO_2$) can swell and plasticize glassy polymers, leading to a depression on their glass-transition temperature (T_g) to almost the same extent as affected by solvents or vapors.[27−30] This remarkable depression in T_g means the increased mobility of polymer chains and hence allows the fast relaxation of polymer chains, resulting in the fast crystallization in the semicrystalline polymers such as poly(aryl ether ether ketone) (PEEK),[29] methyl-substituted PEEK[31] and PC,[32−37] and even the non-thermally crystallizable polymers such as *tert*-butyl PEEK[28] at any temperature between T_g and the degradation temperature. Therefore, the crystallization of PC will occur in $scCO_2$ under milder condition such as low temperature about 75 °C and 20 MPa,[37] which overcomes the time-consuming process of thermal crystallization, thus supplying an effective method for studying the crystallization behavior of PC.

In the present work, the influence of long-chain branching (LCB) on the crystallization behavior of PC in $scCO_2$ was investigated. PCs having similar molecular weights and molecular weight distributions were selected to avoid the influence of polydispersity on crystallization behavior. The free volume in polymer matrix was investigated for the branched and linear PCs by using positron annihilation lifetime spectroscopy (PALS) to clarify the segmental mobility of different chain structure. The influence of LCB on the crystallization behavior of PCs is discussed on the basis of crystallization kinetics, crystallization window in $scCO_2$, and melting thermograms of crystallized samples. The influence of chain structure on the crystal morphology and perfection in crystallized PCs is also discussed.

2. Experimental Section

2.1. Materials and Characterization. A linear bisphenol A polycarbonate (PC-L) and two branched polycarbonates (PC-B1, PC-B2) investigated were supplied as granules by Idemitsu Petrochemical Co (A2700), Bayer (M-3118), and General Electric Plastic (Lexan154), respectively. The characteristics of the PCs studied, such as molecular weight, molecular weight distribution, and T_g, are shown in Table 1. The chemical structure of the different branching agents for PC-Bs is shown in Scheme 1.[17] The incorporation content of branching agents was determined by using base hydrolysis followed by high-performance liquid chromatography, and the results were verified further by ^{1}H NMR measurement. PC-B1 and PC-B2 have about 0.7 branch points/chain, which equals the repeat units per molecule multiplied by the molar content of branching agents (34700/254 × 0.5%). Thus, PC-Bs is star polymers with average M_w/arm higher than 10000 g/mol.[17] CO_2 with a purity of 99.95% was supplied by Beijing Analytical Gas Factory, China. Dichloromethane (DCM) was reagent grade and used as received.

2.2. Sample Preparation. The amorphous thin films were prepared by fast evaporation method suggested by Huang et al.[38] This method avoids crystallization of PC induced by solvent. The 0.5 wt % solution of PC was obtained by dissolving the pellets in DCM and then spin-coating on a heated (about 35 °C) silicon wafer. The obtained films were heated in a vacuum oven for 24 h at 80 °C to remove residual DCM. The amorphous sheets of 0.5 and 2 mm thickness were obtained by compression molding at 250 °C and then quenching in cold water. Differential scanning calorimetry (DSC) measurements indicated that the obtained samples were amorphous.

2.3. $ScCO_2$ Treatments. A high-pressure apparatus was used for the $scCO_2$ treatment. The 0.5 mm thick PC samples and thin films were placed in a high-pressure vessel preheated to the experimental temperature. The vessel was flushed with low-pressure CO_2 for about 3 min and then pressurized to a desired value. Once the CO_2 pressure reached the desired value, the timing began. At the end of the experiment, the vessel was depressurized slowly for preventing the probable foaming of the polymer samples.

2.4. Positron Annihilation Lifetime Spectroscopy (PALS). PALS measurements were performed at room temperature on the 2 mm thick samples by exposing them to the radioactive ^{22}NaCl. The source was sandwiched between two identical specimens (10 × 10 × 2 mm). A fast−fast coincidence circuit of the PALS spectrometer with time resolution of 250 ps as monitored by using a ^{60}Co source was used to record all the PALS spectra. The counting rate was about 70 ps. Each spectrum was collected to a fixed total count of 2×10^6, which was high enough to get a good analysis but at the same time low enough to avoid any substantial radiation effects. All the spectra were analyzed using the program POSITRONFIT.

2.5. Analysis. DSC measurements were carried out to determine the T_g and melting peak (T_m) by using a Perkin-Elmer DSC-7 calibrated with indium. Unless otherwise stated, all scans were made at a heating rate of 10 °C/min in a dry nitrogen environment. The crystallinity degree was calculated from the integration of melting peak of DSC and by using 110.04 J/g for the heat of fusion of 100% crystalline PC.[39] Wide-angle X-ray diffraction (WAXD) measurements were conducted on a Rigaku D/max 2500 with Cu Kα radiation (40 kV, 300 mA). The scanning 2θ angle ranged between 5° and 40° with a step scanning rate of 4° min^{-1}. Imaging of untreated and crystallized PCs thin films treated in $scCO_2$ was performed with an atomic force microscope (AFM) Dimension-3100 (Digital Instrument, Inc.) in the tapping mode at room temperature. Phase images were collected. Silicon tips with constant number of 40 N/m were used.

3. Results and Discussion

3.1. Influence of LCB on the Segmental Mobility of PC. It is well-established that the segmental mobility controls the crystallization rate of polymer, which is mainly involved in the free volume. PALS is utilized as an effective probe to estimate the free volume size and content due to the unique location of the positron and positronium atom (Ps, a bound state consisting of an electron and a positron) in open spaces.[40] In PALS measurements, positrons forming a radioactive source are used to probe the material. When a positron enters a polymer sample, it can annihilate as a free positron in a polymer with a lifetime about 0.3−0.5 ns. The positron can also form a bound state called ortho- and parapositronium (o-Ps and p-Ps, respectively). In p-Ps the spins of the positron and electron are antiparallel, forming a lifetime about 0.12 ns. While in o-Ps the spins of the

Table 2. Free Volume Properties of Untreated PCs

sample	τ_3 (ns)	I_3 (%)	R (Å)	v_f (%)	Δv_f (%)
PC-L	2.01	28.93	2.86	5.11	
PC-B1	2.10	33.91	2.95	5.77	13.1
PC-B2	2.08	30.49	2.92	5.71	11.8

positron and electron are parallel, forming a longer lifetime (about 1−5 ns) than those of p-Ps and free positrons in polymers. In the current PALS method, the observed lifetime of o-Ps, τ_3, is found to be directly correlated to free volume hole size and is determined by eq 1:[41]

$$\tau_3 = \frac{1}{2}\left[1 - \frac{R}{R+\Delta R} + \frac{1}{2\pi}\sin\left(\frac{2\pi R}{R+\Delta R}\right)\right]^{-1} \quad (1)$$

where R is the radius of free volume hole (Å) and ΔR the electron layer thickness, semiempirically determined to be 1.66 Å.

The relative intensity of o-Ps annihilation lifetime, I_3, is related to the free volume hole fraction by the following empirical equation:[42]

$$v_f = AI_3\frac{4}{3}\pi R^3 \quad (2)$$

where v_f is the fraction (%) of the free volume. A is an empirical constant determined from the specific volume data.

The experimental results of τ_3 and I_3 measured for PCs with aging time of 500 h at ambient pressure by PALS are listed in Table 2. The values were 2.01 ns and 28.93% for PC-L, 2.10 ns and 33.91% for PC-B1, and 2.08 ns and 30.49% for PC-B2, respectively. Similar values have also been reported by previously studies.[43−46] It is known that the τ_3 and I_3 are related to the mean free volume size and free volume concentration, respectively. The increase in the τ_3 and I_3 indicates the significant expansion in free volume size and the increase in free volume concentration. R was calculated to be 2.86 (PC-L), 2.95 (PC-B1), and 2.92 Å (PC-B2) from eq 1, which was consistent with the τ_3. With an empirical constant A of 0.0018 for PC,[45] eq 2 yielded the free volume fraction of 5.11 (PC-L), 5.77 (PC-B1), and 5.71% (PC-B2). These results mean that the increase in free volume size and free volume fraction (Δv_f) of 13.1% (PC-B1) and 11.8% (PC-B2) were obtained in branched PCs compared to the linear one. Therefore, the existence of LCB produced larger free volume hole radius and concentration, resulting in the higher free volume fraction in branched PCs than that in the linear one. It is well-established that the free volume cavities are located between polymer chains and at polymer chain ends.[44] This means that the increase in local free volume allows a higher molecular mobility for the branched PCs. As shown in Table 1, the T_g of branched PCs measured by DSC is 3−4 °C lower than that of the linear one. In our previous study,[17] the dielectric relaxation results also showed the branched PC had a low α-relaxation temperature than the linear one. This order was qualitatively consistent with the PALS and DSC measurements in the present study, indicating much higher segmental mobility of branched PCs. Therefore, all these results verified that the substitution of a branch for a linear molecule increased the free volume and decreased T_g, resulting from the increased chain mobility as a result of loosening of the chain packing. Influence of branching structure on the free volume properties was also reported by Kilburn et al.[47] They found that the τ_3 increased from 2.02 ns for poly(methacrylate) to 2.67 ns for poly(*n*-alkyl methacrylate) with six carbon atoms. The same tendency was also observed in I_3 and free volume size. This increase in local free volume allowing a higher segmental mobility was also indicated by the lowering of T_g and a general increase in the frequency of α-relaxation at a given temperature. In branched crystalline polymers such as polypropylene,[48,49] the similar increase in the free volume hole radius and fraction compared to the linear one was also observed. Moreover, accompanying with the increase in side chain length, much larger free volume and fraction could be obtained in the branched polymers. In summary, the LCB in PC leads to the increased segmental mobility of long-chain branched PCs.

3.2. Crystallization Behavior of PCs in $scCO_2$. As mentioned in the Introduction, PC undergoes thermally induced crystallization very slowly, which limits the investigation of crystallization behavior of PC experimentally. The significant plasticization effect of $scCO_2$ increases the segmental mobility of PC[27,50] and enhances the transport process between the amorphous and crystalline phases. Therefore, to conduct the crystallization of PC in $scCO_2$ can shorten the time-consuming process of thermal crystallization. Moreover, CO_2 is easy to be separated with the polymer matrix after depressurization due to the weak intermolecular interactions between CO_2 and polymer. In this section, the effects of LCB on the crystallization kinetics and crystallization window of PC in $scCO_2$ are investigated.

Figure 1 shows the DSC thermograms of PC-L and PC-B2 samples treated by $scCO_2$ at 120 °C and 16 MPa for different times. The choice of PC-B2 as a representative sample of branched PC-Bs was arbitrary as both branched PC samples display a qualitatively similar behavior. PC-L shows only T_g during the DSC heating scan after treating for 4 h, indicating the crystallization did not occur under this condition. The T_g of the treated PC-L sample is 153.9 °C, which was similar to that of untreated one. After the treatment for 6 h, the PC-L exhibits two endotherm peaks during the heating scan, indicating the induced crystallization of PC-L. Comparatively, PC-B2 shows obviously two melting peaks at 4 h. This result suggests that the induction time of crystallization for PC-B2 was much shorter than that of PC-L. It is noted that the treated PC-B2 sample shows an obvious T_g at 151.7 °C, which was slightly higher than 150.8 °C of the untreated one. This result indicates that the existence of crystal region restricted the chain mobility of amorphous region,[51,52] and the related discussion is shown in the following section. With the further increase of treatment time, the intensity of melting peaks increase significantly at 6 h. Compared to PC-L, the induced crystallization of PC-B2 started earlier, indicating the presence of LCB increased the crystallization kinetics of PC.

Figure 2 summarizes the results of crystallinity, obtained from DSC thermograms, of the treated PCs samples. It is shown that the crystallization did not occur for PC-L at 4 h. However, with increasing the treatment time, the crystallinity degree of PC-L increases gradually from 0 to 9.2% and then reaches the equilibrium crystallinity degree at 12 h. The incorporation of branching structure obviously affected the crystallization behavior of PC. PC-B1 and PC-B2 were induced to crystallize at 4 h with crystallinity degree of 1.0 and 2.1%, respectively. With extending the time from 4 to 10 h, there is a significant increase in the crystallinity from 1.0 to 15.9% and from 2.1 to 16.3%, respectively. Further extending the treatment time up to 16 h, the crystallinity of branched PCs becomes independent of treatment time, indicating the equilibrium crystallinity was reached after 10 h. Compared to the linear structure, it is shown clearly that the incorporation of branching structure increased the crystallinity degree and decreased the time to reach the equilibrium crystallinity.

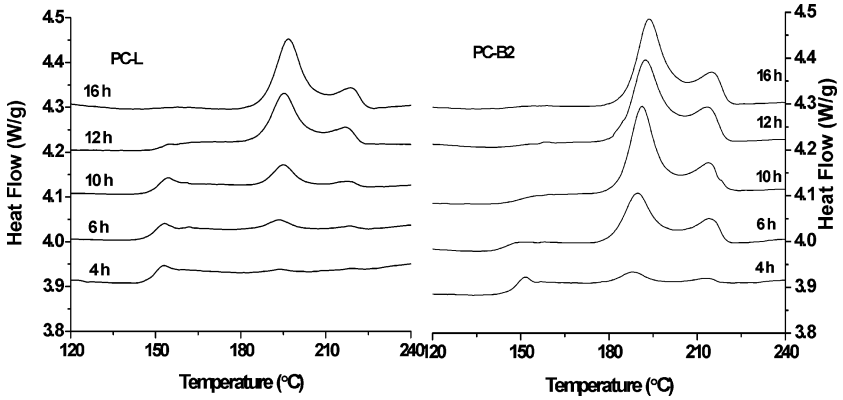

Figure 1. Typical thermograms of treated PC-L and PC-B2 samples at 120 °C and 16 MPa for different time with scan rate of 10 °C/min.

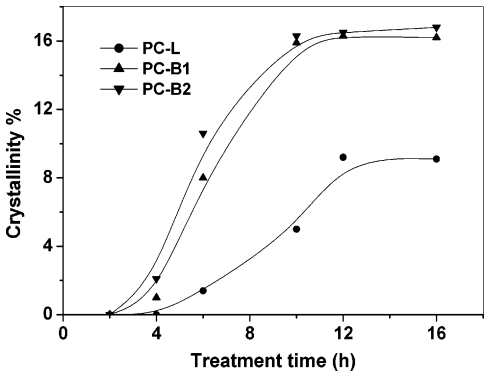

Figure 2. Crystallinity of PCs samples treated at 120 °C and 16 MPa for different time.

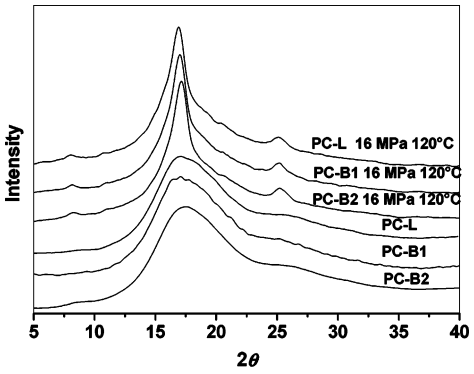

Figure 3. X-ray diffraction patterns of untreated PCs samples and PCs treated at 16 MPa and 120 °C for 12 h.

Typical WAXD results are shown in Figure 3. All untreated samples exhibit a broad diffraction peak at $2\theta = 16.9°$, which indicates that the crystallinity degree in these samples were too low to be detected by WAXD measurements. This phenomenon was agreed well with the results measured by DSC. After being treated by $scCO_2$ at 120 °C and 16 MPa for 12 h, PCs samples present obvious crystalline characteristics and show two diffraction peaks at 16.9° and 25.2°, respectively. These values of 2θ match the monoclinic crystal in the space group C_s^2 of PC identified by Bonart,[53] which means the unit cells of crystal phase in all samples were the same.

A diagram was established to display the general crystallization window of PCs samples in $scCO_2$. The treatment time was fixed in 12 h, which was considered to be enough to induce crystallization of all the PC samples. As shown in Figure 4, three U-shaped curves represent the temperature range of crystallization. Out of the curves the treated PCs are amorphous, while inside are crystallizable. All the three PCs do not

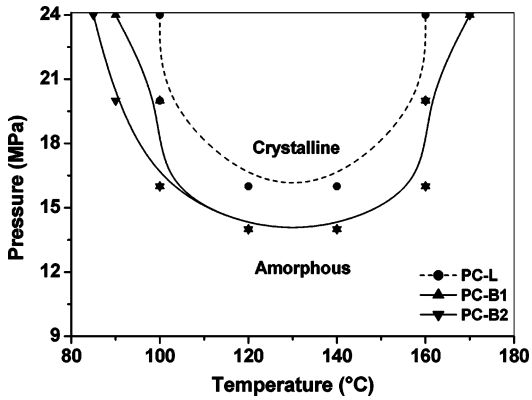

Figure 4. Crystallization window of PCs samples in the presence of $scCO_2$. The treatment time is 12 h.

crystallize at pressures below 12 MPa from 80 to 160 °C in $scCO_2$. At 14 MPa, the branched PC-Bs is induced to crystallize between 120 and 140 °C. With increasing the treatment pressure, the temperature range broadens gradually. At the highest experimental pressure of 24 MPa, PC-Bs are induced to crystallize by $scCO_2$ between 85−90 and 170 °C. The lowest crystallization temperature was similar to our previous results,[35] but higher than 75 °C reported by Beckman et al.,[37] which was attributed to the difference in molecular structure and molecular weight.[33] Compared with the branched PCs, the linear one shows a high-pressure threshold, i.e., 14 MPa, for crystallization, and a narrower range of crystallization, i.e., 100−160 °C. These results indicate that the branched PCs were induced to crystallize in a broadened crystallization window with the incorporation of branching structure.

It is known that the crystallization behavior of PC depends on the molecular weight and molecular weight distribution.[51] In the presence study, the PCs used for $scCO_2$-induced crystallization have similar molecular weight and molecular weight distribution, which offers the possibility to study the influence of LCB on crystallization behavior of PC. It is well-established that an increase in polymer segmental mobility would be an effective route to the enhancement of polymer crystallization. PLAS measurements shown above indicate that the LCB increased the size of holes and content of free volume, resulting in the enhancement in segmental mobility. This increase decreased the crystallization barrier and hence tended to increase the crystallization rate and broadened the crystallization temperature. In other words, the presence of LCB was kinetically favorable for PC crystallization. The similar increase in crystallization rate was also observed in branched poly(ethylene terephthalate) with branching agent of 0.4−0.8 mol % by a thermal crystallization process compared to the linear one.[7] At

high concentration of branching (1.4−5.0 mol %), however, the molecular entanglement reduced segmental mobility and hence diminished the crystallization rate.[6] In our study, the branching concentration of 0.5 mol % facilitated the crystallization of PC-Bs in $scCO_2$ resulted from the increased segmental mobility with the incorporation of branching structure. Moreover, it is noted that the highest temperature of crystallization was 170 °C for branched PCs, contrary to 160 °C for linear PC, which means that the branched PCs could be induced to crystallize at higher temperatures. This apparent broadening of the crystallization window for the branched PCs was possibly a consequence of a stronger effect of branching structure on segmental mobility than crystallization driving force. This observation is in accordance with the results of Alizadeh et al.,[51] who noted the crystallization window of PC became broader with decreasing the molecular weight.

3.3. Influence of Treatment Conditions on the Melting Behavior of PCs. When a polymer crystallizes, the crystals grow from individual nuclei. The chains fold and grow in three dimensions to form lamellar. It is shown in Figure 1 that the crystallized PC shows two melting peaks, a low melting temperature (T_{m1}) and a high melting temperature (T_{m2}), during the DSC heating scan, which are associated with the melting of two distinct populations of crystals with different thermal stability.[54,55] T_{m2} is related to the melting of lamellae formed during the primary crystallization process, while T_{m1} to those formed during the secondary crystallization process.[36,51,54] According to the X-ray diffraction results (Figure 3) of the corresponding samples, the double melting behavior did not result from the different crystal types. In the following section, the origin and change of T_{m1} and T_{m2} will be investigated at different scan rate, treatment time, pressure, and temperature. On the basis of these results, a discussion will be made on the influence of LCB on the crystal morphology and perfection in treated PCs.

3.3.1. Influence of Scan Rate. PCs samples were treated by $scCO_2$ at 20 MPa and different temperatures for 12 h and then heated with scanning rate from 5 to 20 °C/min. T_{m2} and T_{m1} are plotted as a function of the square root of heating rate $\beta^{1/2}$, as shown in Figure 5. It is seen that T_{m2} is independent of heating rate within experimental error, that is, for PC-L 211.2 ± 0.2 °C at 100 °C, 216.6 ± 0.3 °C at 120 °C, and 223.0 ± 0.1 °C at 140 °C, while for PC-Bs 209.5 ± 0.1 °C at 100 °C, 214.6 ± 0.2 °C at 120 °C, and 221.0 ± 0.2 °C at 140 °C. This result means that the T_{m2} did not increase from the reorganization process taking place during heating.[51,54] It is known that primary crystallization results from a completely unconstrained melt, which generally needs much large driving force toward crystal formation. Therefore, the crystallites related to the T_{m2} possess high stability and perfection.

Figure 5 shows that T_{m1} increases linearly with $\beta^{1/2}$, that is, for PC-L treated at 100 °C from 185.9 °C at 5 °C/min to 191.9 °C at 20 °C/min, at 120 °C from 195.0 to 201.5 °C, and at 140 °C from 204.7 to 211.0 °C, with an average slope of 2.5 ± 0.1 °C/(°C/min)$^{1/2}$. For PC-Bs treated at 100 °C from 183.6 °C at 5 °C/min to 189.4 °C at 20 °C/min, at 120 °C from 193.0 to 199.3 °C, and at 140 °C from 202.3 to 209.0 °C, with an average slope of 2.5 ± 0.1 °C/(°C/min)$^{1/2}$. The same slope obtained for PC-L and PC-Bs at various treatment temperatures indicates that the crystals related to T_{m1} showed similarly a superheating behavior.[56] Marand et al.[51,54] verified this superheating behavior was incompatible with the concept of a multiple melting behavior by a melting−recrystallization−remelting process. Rather, it was a consequence of a decrease in conformational entropy of the remaining amorphous fraction. This decrease in conformational entropy resulted in the secondary crystallization. Therefore, the secondary crystallization was a local phenomenon which involves a section of a given chain, and the crystallization regions was only limited in the direct vicinity of primary lamellar crystals.[51] Our present study also verified the origin of secondary crystallization based on two reasons as follows. One was the increased T_g's of crystallized PC samples compared to the amorphous one as mentioned before. The increase in T_g indicates an increase in the level of conformational constraint in the amorphous fraction when crystallization occurred.[43,44] On the other hand, the double melting peaks of crystallized PC samples at 120 °C and 20 MPa with different scan rates were curve-fitted by Peakfit v4.1, and the results are shown in Table 3. It is clear that the crystallinity ratio of secondary crystallization vs the total ratio, i.e., $X_{c1}/X_{c\ total}$, increases gradually as a function of $\beta^{1/2}$. This result means that the crystallinity associated with the T_{m1} increased with increasing $\beta^{1/2}$. This observed behavior was consistent with T_{m1}. Therefore, T_{m1} was related to melting of lamellae formed during the secondary crystallization process, which resulted from the topological constraints in the residual amorphous fraction, and showed lower stability and perfection than that of T_{m2}.

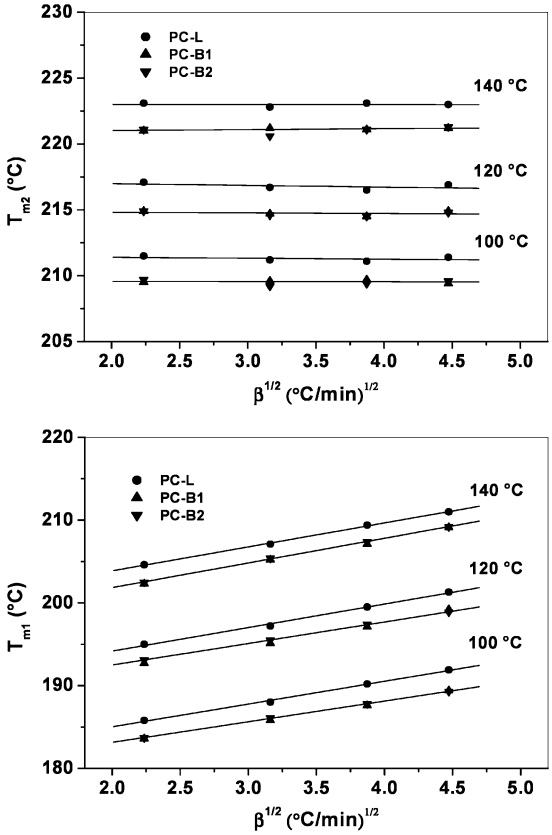

Figure 5. Plots of T_{m2} and T_{m1} vs square root of scan rate $\beta^{1/2}$ of PCs samples treated at different temperatures and 20 MPa for 12 h.

Table 3. X_{c1}/X_{ctotal} of PCs Samples Treated at 120 °C and 20 MPa with Different Scanning Rate

	β (°C/min)			
sample	5	10	15	20
PC-L	62.4	75.9	84.2	91.6
PC-B1	53.1	69.2	73.1	82.5
PC-B2	54.3	67.4	71.5	81.5

3.3.2. Influence of Treatment Time. Figure 6 shows the different dependence of T_{m2} and T_{m1} on the treatment time at 120 °C and 16 MPa. For PC-L T_{m2} is 217.4 ± 0.3 °C and for

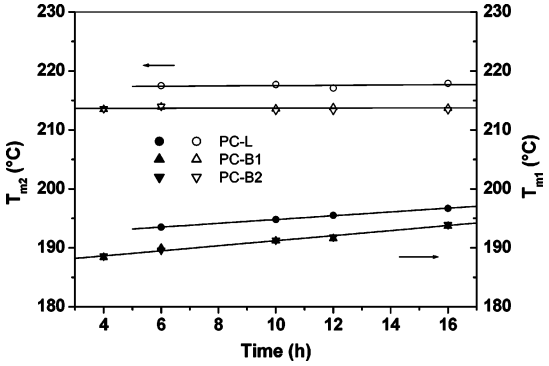

Figure 6. Plots of T_{m2} and T_{m1} vs treatment time of PCs samples treated at 120 °C and 16 MPa.

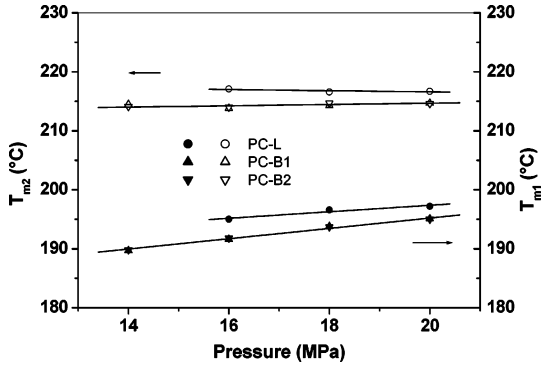

Figure 7. Plots of T_{m2} and T_{m1} vs CO_2 pressure for PCs samples treated at 120 °C for 12 h.

PC-Bs 214.2 ± 0.5 °C, showing no shift with increasing treatment time. Different from this, T_{m1} increases linearly with increasing time. For PC-L it increases from 193.5 °C for 6 h to 196.8 °C for 16 h with a slope of 0.37 °C/h, while for PC-Bs from 188.4 °C for 4 h to 193.5 °C for 16 h with a slope of 0.44 °C/h. A similar phenomenon has been observed in PC[36,51] and other semicrystalline polymers such as poly(ether ether ketone).[52,57,58] These phenomena indicate that the lamellae formed during the primary crystallization process do not thicken with increasing the treatment time in the temperature range investigated, while more significant crystallization regions are formed at longer treatment time during the secondary crystallization. It is known that the primary crystallization exhibits much longer induction time and develops before the secondary crystallization.[51,52,58] Therefore, in the present study the unchanged T_{m2} with increasing the treatment time suggests the primary lamellae were developed completely when the secondary crystallization was taking place. This increase in T_{m1} was qualitatively consistent with the increased crystallinity of PCs at extended treatment time (Figure 2), indicating the increased conformational constraint in the remaining amorphous phase at longer treatment time.

3.3.3. Influence of CO_2 Pressure. Figure 7 shows the change of T_{m2} and T_{m1} as a function of CO_2 pressure at 120 °C for 12 h. T_{m2} is independent of CO_2 pressure, that is, for PC-L 217.0 ± 0.3 °C and for PC-Bs 214.0 ± 0.4 °C. On the contrary, T_{m1} shifts linearly toward higher temperatures with increasing CO_2 pressure, i.e., for PC-L from 195.0 °C at 16 MPa to 197.5 °C at 20 MPa with a slope of 0.67 °C/MPa, while for PC-Bs from 189.5 °C at 14 MPa to 195.0 °C at 20 MPa with a slope of 0.83 °C/MPa. These results indicate that the lamellar perfection of primary crystallites was not improved by increasing CO_2 pressure. It is known that an increase in CO_2 pressure tends to increase the mobility of polymer chains and lower T_g. Therefore, the transformation of the amorphous phase of the polymer to a lower free energy crystalline structure is kinetically favorable. However, the increased CO_2 pressure did not affect obviously crystallization thermodynamics of PC. A possible reason is that the compact crystallite structure restricted the solubility of CO_2 in crystal region, which decreased the effect of CO_2 pressure on crystalline thermodynamics. The T_{m1} is associated with the melting of secondary crystallite. An increase in CO_2 pressure tended to increase the mobility activity of amorphous fraction, which facilitated the regular arrangement of polymer chain, resulting in an increase in T_{m1}.

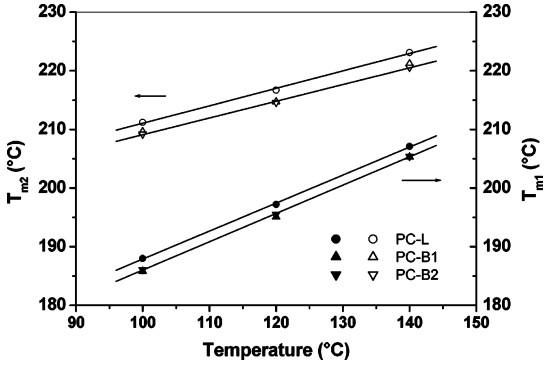

Figure 8. Plots of T_{m2} and T_{m1} vs treatment temperature for PCs samples treated at 20 MPa for 12 h.

3.3.4. Influence of Treatment Temperature. In Figure 8, both T_{m2} and T_{m1} of PCs increase linearly with increasing treatment temperature at 20 MPa. For PC-L T_{m2} increases from 211.1 °C at 100 °C to 223.2 °C at 140 °C with a slope of 0.30 °C/°C, while for PC-Bs from 209.0 to 220.7 °C with a slope of 0.29 °C/°C. For PC-L T_{m1} increases from 188.2 at 100 °C to 207.1 °C at 140 °C with a slope of 0.47 °C/°C, while for PC-Bs from 185.8 to 205.4 °C with a slope of 0.49 °C/°C, respectively. These results indicate that the treatment temperature showed obvious different effects on double melting peaks compared to scanning rate, treatment time, and CO_2 pressure. It is known that the increase in the treatment temperature tends to enhance the chain mobility of polymer, which facilitates the arrangement of polymer chains in crystal region, indicating the lamellar thickening at higher temperature. Therefore, an increase in treatment temperature was both kinetically and thermodynamically favorable for PC crystallization in our experimental scopes. Note that the slope of T_{m1} vs treatment temperature of PCs is larger than that of T_{m2}, which indicates that the lamellar thickening process of secondary crystal was more sensitive to the treatment temperature compared to that of primary crystal. A possible reason is that the enhanced primary crystallization further increased the conformational constraints of the remaining amorphous phase,[36,51] resulting in a large increase in secondary crystallization.

3.4. Influence of LCB on the Melting Behavior of PCs. In Figures 6−8, $scCO_2$-induced crystallization of PCs at different treatment times, pressures, and temperatures are characterized by double melting peaks. Under all these experimental conditions, the T_{m2} and T_{m1} of PC-Bs were about 2−4 °C lower than those of PC-L. These results indicate that the melting of primary and secondary crystals of PC-Bs occurred at lower temperatures compared to those of PC-L. It has been shown above that the upward shift in T_{m2} is related to an increase in crystal perfection or a crystal thickening process. Therefore, the incorporation of branching structure disturbed thickening of the crystallites or increased the lattice disorder of the formed crystallites in branched PC. On the other hand, higher T_{m1} of PC-L was

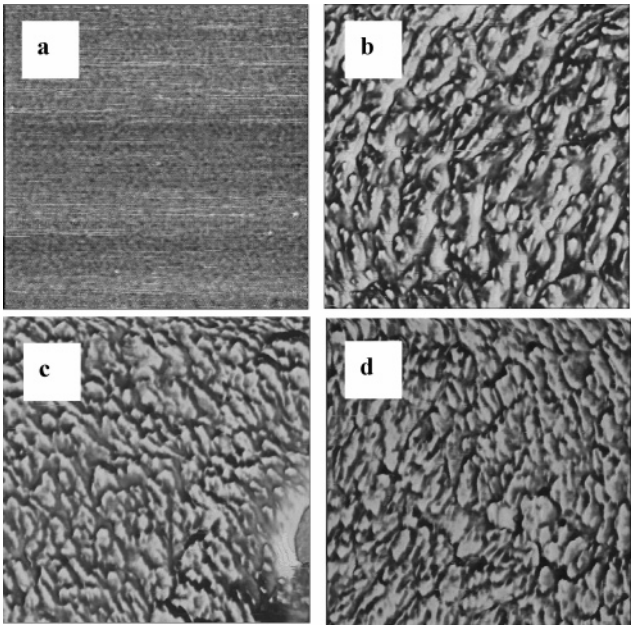

Figure 9. AFM phase images of untreated PC-L and crystallized PCs treated at 120 °C and 20 MPa for 12 h: (a) pure PC-L 1 × 1 μm; (b) crystallized PC-L 1 × 1 μm; (c) crystallized PC-B1 1 × 1 μm; (d) crystallized PC-B2 1 × 1 μm.

Table 4. Fibrillar Size of Crystallized PCs Samples Treated at 120 °C and 20 MPa for 12 h

	fibrillar thickness (nm)		fibrillar length (nm)	
sample	d	$\bar{d}$	l	$\bar{l}$
PC-L	18−66	41	100−500	230
PC-B1	10−57	37	100−300	150
PC-B2	10−60	40	100−200	145

observed at different treatment conditions, resulting from the much larger increase in topological constraints of the remaining phase due to the enhanced primary crystallization process.[51]

Now the issue is the influence of the LCB on the crystal morphology. It is well-established that the atomic force microscope (AFM) phase imaging supplies a popular technique to investigate the crystal morphology of polymer. In this study, AFM technique was used to further investigate the effect of LCB on crystal morphology. Figure 9 shows a typical set of AFM micrographs of untreated PC-L and $scCO_2$-treated PCs at 120 °C and 20 MPa for 12 h. In these micrographs the lighter regions are associated with the crystalline phase and the darker regions with the amorphous phase. The main components of crystallized PC-L are numerous fibrillar nanocrystallites associated with lamellar growth, and some little crystals exist among the fibrillar crystal. With the presence of branching structure in PC, the length of nanocrystallites decreases gradually, while the breadth does not decreases obviously. For a more quantitative analysis, the size of nanocrystallites was measured from the AFM micrographs and summarized in Table 4. The average thickness and length are 41 and 230 nm for PC-L, 37 and 150 nm for PC-B1, and 40 and 145 nm for PC-B2. These results provide a strong support for high perfection of crystallites of PC-L compared to the branched PCs under the same treatment conditions, which was qualitatively consistent with the T_{m2} of DSC measurements (Figure 5). Therefore, the development of crystallization was more perfect in three-dimension for PC-L than for PC-Bs. This phenomenon has also been observed for poly(L-lactic acid)[8] and other polyester systems.[7,10]

It is noted that there were higher crystallite densities of PC-Bs than that of PC-L in AFM micrographs. This increased crystal density in PC-Bs was in agreement with the result of crystallinity via DSC measurement. These phenomena suggest that these LCB units were acting as nucleating sites in the crystallization process. As shown in experimental section, the average M_w of long chain branch for PC-Bs was higher than 10 000 g/mol. This value was much greater than the critical molecular weight for entanglement, M_c, e.g. 1200−1400,[59] 4000,[60] or 4800 g/mol,[61] and hence the branch chain of PC-B molecules was able to crystallize.[5] The crystals formed by branch chains may supply the nucleation sites for crystallization. Thus, in the branched PCs, the probability of the system to nucleate was enhanced, leading to an increase in the crystal density or crystallinity degree. Similar behavior has been reported for other polymers,[6,62] where the crystallinity was significantly increased with introducing the long branch in polymer.

4. Conclusions

The influence of LCB on crystallization behavior of PC and double melting peaks of crystallized PC has been investigated. The selection of $scCO_2$ as a combining severe environment was attributed to its strong plasticization effect and environmentally benign character. The linear and branched polycarbonates have the similar molecular weight and molecular weight distribution; therefore, the effect of polydispersity on crystallization behavior does not need to take into consideration. The PALS results indicate that the branched PCs had much more free volume than that of the linear one. This increase in segmental mobility decreased the energy barrier for PC crystallization. Therefore, in the presence of $scCO_2$, branched PCs exhibited much quicker crystallization rate and broader crystallization window compared to the linear PC. Studies of the heating rate dependence of the melting behavior of crystallized PC indicate that the T_{m2} and T_{m1} were associated with the melting of primary and secondary crystallization, respectively. DSC measurements showed that the T_{m2} of PC-Bs was about 2−4 °C lower than that of PC-L at the same treatment time, pressure, and temperature. This result, accompanied by the much large crystal size for PC-L observed by AFM, suggests that the incorporation of LCB decreased the perfection or increased the lattice disorder of primary crystallites. The T_{m1} of crystallized PC-Bs was also much lower than that of PC-L under the same treatment conditions, which attributed to the decrease in primary crystallization process resulting in the reduced conformational constraints in the residual amorphous regions. AFM results also indicate that the branching structure might acted as nucleating sites to increase the crystallinity of PC.

Acknowledgment. This work was supported by the National Natural Science Foundation of China (Grants 20574082 and 20274056).

References and Notes

(1) Mandelkern, L. *Crystallization of Polymers*; McGraw-Hill: New York, 1964.
(2) Watson, M. D.; Wagener, K. B. *Macromolecules* **2000**, *33*, 8963−70.
(3) Smith, J. A.; Brzezinska, K. R.; Valenti, D. J.; Wagener, K. B. *Macromolecules* **2000**, *33*, 3781−94.
(4) Qiu, W.; Sworen, J.; Pyda, M.; Nowak-Pyda, E.; Habenschuss, A.; Wagener, K. B.; Wunderlich, B. *Macromolecules* **2006**, *39*, 204−17.
(5) McKee, M. G.; Unal, S.; Wilkes, G. L.; Long, T. E. *Prog. Polym. Sci.* **2005**, *30*, 507−39.
(6) Jayakannan, M.; Ramakrishnan, S. *J. Appl. Polym. Sci.* **1999**, *74*, 59−66.
(7) Li, G.; Yang, S. L.; Jiang, J. M.; Wu, C. X. *Polymer* **2005**, *46*, 11142−8.

(8) Tsuji, H.; Miyase, T.; Tezuka, Y.; Saha, S. K. *Biomacromolecules* **2005**, *6*, 244−54.
(9) Kulinski, Z.; Piorkowska, E. *Polymer* **2005**, *46*, 10290−300.
(10) Wang, J. L.; Dong, C. M. *Polymer* **2006**, *47*, 3218−28.
(11) Núñez, E.; Ferrando, C.; Malmström, E.; Claesson, H.; Werner, P. E.; Gedde, U. W. *Polymer* **2004**, *45*, 5251−63.
(12) Kricheldorf, H. R.; Domschke, A. *Macromolecules* **1994**, *27*, 1509−16.
(13) Acierno, S.; Van Puyvelde, P. *Polymer* **2005**, *46*, 10331−8.
(14) Duran, R.; Ballauff, M.; Wenzel, M.; Wegner, G. *Macromolecules* **1988**, *21*, 2897−99.
(15) Chen, S. A.; Ni, J. M. *Macromolecules* **1992**, *25*, 6081−9.
(16) Hsu, W. P.; Levon, K.; Ho, K. S.; Myerson, A. S.; Kwei, T. K. *Macromolecules* **1993**, *26*, 1318−23.
(17) Liu, C. Y.; Li, C. X.; Chen, P.; He, J. S.; Fan, Q. R. *Polymer* **2004**, *45*, 2803−12.
(18) Zhang, X.; Li, Z.; Lu, Z.; Sun, C. C. *Macromolecules* **2002**, *35*, 106−11.
(19) Kim, M. H.; Phillips, P. J. *J. Appl. Polym. Sci.* **1998**, *70*, 1893−905.
(20) Russell, K. E.; McFaddin, D. C.; Hunter, B. K.; Heyding, R. D. *J. Polym. Sci., Part B: Polym. Phys.* **1996**, *34*, 2447−58.
(21) Greenberg, S. A.; Alfrey, T. *J. Am. Chem. Soc.* **1954**, *76*, 6280−5.
(22) Hempel, E.; Huth, H.; Beiner, M. *Thermochim. Acta* **2003**, *403*, 105−14.
(23) Turska, E.; Przygocki, W.; Masławski, M. *J. Polym. Sci., Part C: Polym. Symp.* **1968**, *16*, 3373−7.
(24) Schnell, H. *Chemistry and Physics of Polycarbonates*; Interscience: New York, 1964.
(25) Moore, W. R.; Sheldon, R. P. *Polymer* **1961**, *2*, 315−21.
(26) Kambour, R. P.; Gruner, C. L.; Romagosa, E. E. *Macromolecules* **1974**, *7*, 248−53.
(27) Zhang, Z. Y.; Handa, Y. P. *J. Polym. Sci., Part B: Polym. Phys.* **1998**, *36*, 977−82.
(28) Handa, Y. P.; Zhang, Z. Y.; Roovers, J. *J. Polym. Sci., Part B: Polym. Phys.* **2001**, *39*, 1505−12.
(29) Handa, Y. P.; Capowski, S.; O'Neill, M. *Thermochim. Acta* **1993**, *226*, 177−85.
(30) Zhang, Z.; Handa, Y. P. *Macromolecules* **1997**, *30*, 8505−7.
(31) Handa, Y. P.; Roovers, J.; Wang, F. *Macromolecules* **1994**, *27*, 5511−6.
(32) Shi, C. M.; DeSimone, J. M.; Kiserow, D. J.; Roberts, G. W. *Macromolecules* **2001**, *34*, 7744−50.
(33) Gross, S. M.; Roberts, G. W.; Kiserow, D. J.; Desimone, J. M. *Macromolecules* **2000**, *33*, 40−5.
(34) Gross, S. M.; Flowers, D.; Roberts, G. W.; Kiserow, D. J.; DeSimone, J. M. *Macromolecules* **1999**, *32*, 3167−9.
(35) Liao, X.; Wang, J.; Li, G.; He, J. S. *J. Polym. Sci., Part B: Polym. Phys.* **2004**, *42*, 280−5.
(36) Hu, X.; Lesser, A. J. *Polymer* **2004**, *45*, 2333−40.
(37) Beckman, E.; Porter, R. S. *J. Polym. Sci., Part B: Polym. Phys.* **1987**, *25*, 1511−7.
(38) Huang, D.; Yang, Y.; Zhuang, G.; Li, B. *Macromolecules* **1999**, *32*, 6675−8.
(39) Mercier, J. P.; Legras, R. *J. Polym. Sci., Polym. Lett.* **1970**, *8*, 645−50.
(40) Jean, Y. C. In *Positron Spectroscopy of Solid*; Dupasquier, A., Mills, A. P., Jr., Eds.; ISO: Ohmsha, 1995; p 563.
(41) Eldrup, M.; Lightbody, J.; Sherwood, J. N. *Chem. Phys.* **1981**, *63*, 51−8.
(42) Kobayashi, Y.; Zhang, W.; Meyer, E. F.; McGervey, J. D.; Jamieson, A. M.; Simha, R. *Macromolecules* **1989**, *22*, 2302−6.
(43) Hristov, H. A.; Bolan, B.; Yee, A. F.; Xie, L.; Gidley, D. W. *Macromolecules* **1996**, *29*, 8507−16.
(44) Liu, L. B.; Gidley, D.; Yee, A. F. *J. Polym. Sci., Part B: Polym. Phys.* **1992**, *30*, 231−8.
(45) Hong, X.; Jean, Y. C.; Yang, H.; Jordan, S. S.; Koros, W. J. *Macromolecules* **1996**, *29*, 7859−64.
(46) Cangialosi, D.; Schut, H.; van Veen, A.; Picken, S. J. *Macromolecules* **2003**, *36*, 142−7.
(47) Kilburn, D.; Dlubek, G.; Pionteck, J.; Alam, A. M. *Polymer* **2006**, *47*, 7774−85.
(48) Bamford, D.; Dlubek, G.; Lüpke, T.; Kilburn, D.; Stejny, J.; Menke, T. J.; Alam, A. M. *Macromol. Chem. Phys.* **2006**, *207*, 492−502.
(49) Dlubek, G.; Bamford, D.; Rodriguez-Gonzalez, A.; Bornemann, S.; Stejny, J.; Schade, B.; Alam, M. A.; Arnold, M. *J. Polym. Sci., Part B: Polym. Phys.* **2002**, *40*, 434−53.
(50) Alessi, P.; Cortesi, A.; Kikic, I.; Vecchione, F. *J. Appl. Polym. Sci.* **2003**, *88*, 2189−93.
(51) Alizadeh, A.; Sohn, S.; Quinn, J.; Marand, H. *Macromolecules* **2001**, *34*, 4066−78.
(52) Marand, H.; Alizadeh, A.; Farmer, R.; Desai, R.; Velikov, V. *Macromolecules* **2000**, *33*, 3392−403.
(53) Bonart, V. R. *Makromol. Chem.* **1966**, *92*, 149−69.
(54) Sohn, S.; Alizadeh, A.; Marand, H. *Polymer* **2000**, *41*, 8879−86.
(55) Chung, J. S.; Cebe, P. *Polymer* **1992**, *33*, 2312−24.
(56) Schawe, J. E. K.; Strobl, G. R. *Polymer* **1998**, *39*, 3745−51.
(57) Cheng, S. Z. D.; Cao, M. Y.; Wunderlich, B. *Macromolecules* **1986**, *19*, 1868−76.
(58) Verma, R.; Marand, H.; Hsiao, B. *Macromolecules* **1996**, *29*, 7767−75.
(59) León, S.; van der Vegt, N.; Delle Site, L.; Kremer, K. *Macromolecules* **2005**, *38*, 8078−92.
(60) Wimberger-Friedl, R.; Hut, M. G. T.; Schoo, H. F. M. *Macromolecules* **1996**, *29*, 5453−8.
(61) Wool, R. P. *Macromolecules* **1993**, *26*, 1564−9.
(62) Gopakumar, T. G.; Ghadage, R. S.; Ponrathnam, S.; Rajan, C. R.; Fradet, A. *Polymer* **1997**, *38*, 2209−14.

MA062181G